

Effect of features extraction on improving LSTM network quality in ECG signal classification

Abstract. This article focuses on the extraction of features extracted from ECG measurement signals to improve the quality of LSTM network operation. Two features were distinguished from each individual sequence of ECG signals: instantaneous frequency (IF) and spectral entropy (SE). Both of these features are extracted from ECG signals using short-time Fourier transform. The applied approach enables the conversion of original measurement sequences into spectral images, from which IF and SE coefficients are then generated. As a result of the research, it was found that feature extraction significantly improves ECG signal classification both in terms of forecasting accuracy and in terms of network learning speed.

Streszczenie. W niniejszym artykule skupiono się na ekstrakcji cech wyodrębnionych z sygnałów pomiarowych EKG w celu poprawy jakości działania sieci LSTM. Z każdej indywidualnej sekwencji sygnałów EKG wyróżniono dwie cechy: częstotliwość chwilową (IF) i entropię widmową (SE). Obie te cechy są wyodrębniane z sygnałów EKG przy użyciu krótkotrwałej transformaty Fouriera. Zastosowane podejście umożliwia konwersję oryginalnych sekwencji pomiarowych na obrazy widmowe, z których następnie generowane są współczynniki IF i SE. W wyniku badań stwierdzono, że ekstrakcja cech znacząco poprawia klasyfikację sygnału EKG zarówno pod względem dokładności prognozowania, jak i szybkości uczenia się sieci. (Wpływ ekstrakcji cech na poprawę jakości sieci LSTM w klasyfikacji sygnału EKG).

Keywords: ECG signal classification, artificial neural networks, machine learning, time series analysis.

Słowa kluczowe: klasyfikacja sygnałów EKG, sztuczne sieci neuronowe, uczenie maszynowe, analiza szeregów czasowych..

Introduction

Over the past 20 years there has been a clear increase in the requirements for disease diagnostics software [1]. In addition to such features as reliability, efficiency or speed of operation, its automation has become an important determinant of the quality of medical software [2]. Automation is necessary for the development of technologies such as Internet of Things (IoT) [3], Body Sensor Network (BSN) [4] or Wearable Textronic Devices (WTD) [5]. IoT not only enables mutual machine-machine communication, but also has the ability to make autonomous decisions by devices. BSN systems operate on the basis of IoT. In turn, WTDs are necessary for the continuous and independent of visits to the doctor's office to collect data directly from the patient's body. As you can see, all these systems interpenetrate each other, creating a holistic environment whose key element is sensors and medical diagnostic software.

ECG signal classification algorithms are an extremely important part of such software [1], [6]. Since cardiovascular disease is one of the leading causes of death in both the US and the world, effective diagnosis of heart disease is a must. It was noticed many years ago that time series or ECG measurement sequences can be classified using statistical or iterative methods [7]. However, the quality of these classifications was not sufficient to eliminate a doctor from the ECG signal interpretation process or, in other words, the diagnosis of the disease [5]. Without the need to involve a doctor, there can be no question of a real automation of the diagnostic process. To enable this, it is necessary to create a reliable cyberphysical system, equipped with sensors and an algorithm, generating repeatable results with 100% accuracy [8].

This article carried out research aimed at obtaining high-quality results of ECG signal classification using the LSTM network. It was assumed that the barrier preventing the training of high accuracy LSTM networks is data. Due to their noise and lack of full repeatability caused by various types of measurement disturbances and inaccuracy of the equipment used, the use of direct data makes it impossible to train the LSTM network with the desired accuracy of prediction. Therefore, the feature extraction method was

used. Two features were distinguished from each single ECG signal sequence: instantaneous frequency (IF) and spectral entropy (SE). Spectrograms and short-time Fourier transform were used for this purpose. The LSTM network was trained both on the basis of direct measurements and on the basis of extracted IF and SE features. The obtained results clearly proved that in the examined cases the extraction of features enabled achieving full, 100% accuracy of classification, while the accuracy of classification for the raw ECG data was about 20% worse.

Materials and methods

There are many methods for solving complex algorithmic problems [9-24]. The research used the LSTM network consisting of 5 layers. The first layer contains single measurement sequences (first variant) or double sequences of the extracted features: IF and SE (second variant). The second layer in both variants contains 150 hidden neurons (activations). The third layer of BiLSTM has 128 hidden units. Layer four is a fully connected layer. It contains six binary neurons because there are so many classes identified by the LSTM network. The fifth layer is of the softmax type. Formula (1) shows the softmax activation function

(1)

$$y_r(x) = e^{a_r(x)} / \sum_{j=1}^k e^{a_j(x)}$$

where $0 \leq y_r \leq 1$ and $\sum_{j=1}^k y_j = 1$.

The last layer is the classification layer, which task is to calculate the cross entropy loss for classification problem with mutually exclusive classes. As a result of feature extraction, a single ECG signal sequence was replaced with two IF and SE sequences. Table 1 shows the structure of the LSTM network used, detailing the individual layers, numbers of activations, weights and biases. Figure 1 shows 6 different classes of ECG signals, including 1 normal rhythm and 5 diseased. Figure 2 shows the same signals but in the form of an extracted IF feature. It can be seen that the transformed signals are significantly different from

the raw ECG signals. First of all, they are devoid of a large number of irrelevant details that make it difficult to correctly classify and interpret characteristic, repetitive sequences.

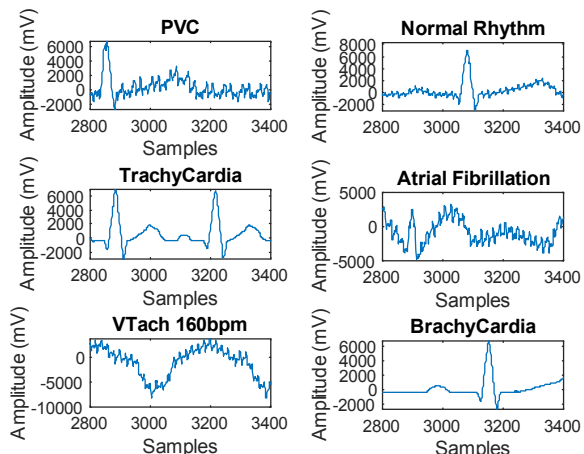


Fig. 1. Raw ECG signals waveforms

When comparing Figures 1 and 2, it is worth paying attention to the horizontal axes. Each of the ECG signals had a frequency of 1,000 Hz and a duration of 5 seconds, resulting in 5,000 measurements. The transformation of the ECG signal into IF significantly reduced the number of measurements. From each signal of 5,000 measurements, 2 signals (IF and SE) with a length of 129 measurements were obtained.

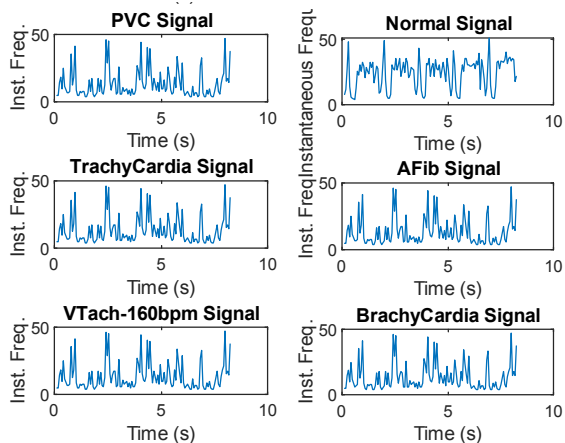


Fig. 2. Instantaneous frequency (IF) for each type of ECG signal

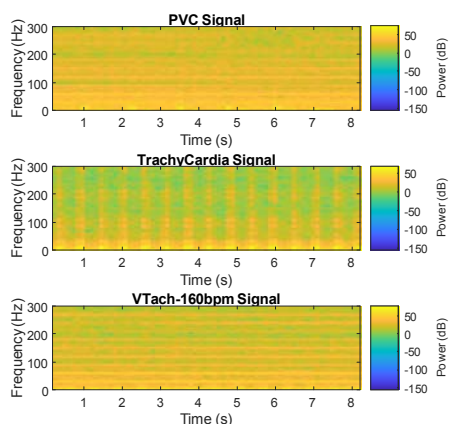


Fig. 3. Examples of ECG signal spectrograms

Figure 3 shows 3 sample ECG signal spectrograms for cardiovascular diseases such as PVC, Trachycardia, and VTach-160bpm. The differences in images visible to the

naked eye are of paramount importance for the effectiveness and legitimacy of applying a deep neural network to this problem. It is well known that convolutional neural networks, which also include LSTM networks, work well in dealing with image classification problems. By transforming the signal into a 2D image, we can make better use of the properties of the LSTM network. Especially that such networks, due to their long-term and short-term memory, are particularly suitable for solving time series and signal prediction problems.

Figures 4 and 5 show the LSTM network training graphs for unprocessed inputs, while Figures 6 and 7 show the same graphs but for the inputs transformed into 2 features extracted - IF and SE. It is clearly seen that the LSTM network trains better in the second variant, when the inputs are features extracted generated as based on a short-time Fourier transform. The quality assessment of the LSTM network training process was based on two indicators - accuracy and loss. The accuracy indicator is described by the firm formula (2)

$$(2) \quad Acc = \frac{K_c}{K} \cdot 100\%$$

where: K_c – number of pixels reconstructed correctly, K – total number of pixels.

The loss indicator is described by the formula (3)

$$(3) \quad Loss = - \sum_{i=1}^N P_i \log(Y_i) / K$$

where: K – number of observations, N – number of responses, P_i – patterns, Y_i – outputs.

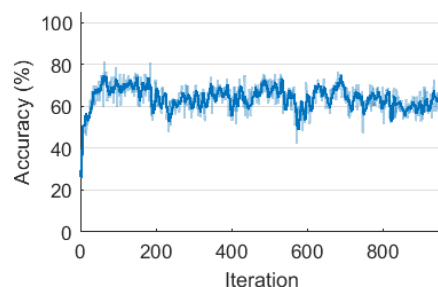


Fig. 4. Training accuracy with a raw signal

The quality of the LSTM network is the better the higher the accuracy and the lower the loss. In Figure 4 accuracy cannot exceed 80% and loss cannot fall below 0.5. Figures 5 and 7 look quite different, where the training of the LSTM network after converting a single input, which is the raw EKG signal into a double sequence of IF (instantaneous frequency) and SE (spectral entropy) signals.

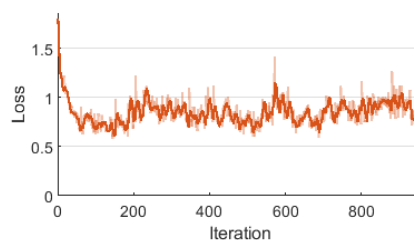


Fig. 5. Training loss with a raw signal

After the features are extracted, a similar LSTM network is able to achieve an accuracy of 100% and a loss of 0. Also, the shape of the training curve indicates its correct course.

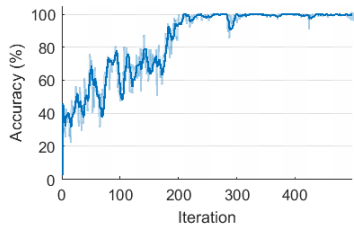


Fig. 6. Training accuracy with IF and SE as input

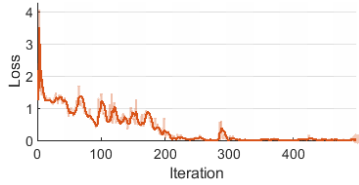


Fig. 7. Training loss with IF and SE as input

Table 1. Layers of LSTM neural network

Layer #	Layer description	Activations	Learnable parameters (weights and biases)
1	Sequence input with 2 dimensions (IF and SE)	2	–
2	BiLSTM with 150 hidden units	300	Input weights: 1200×2; Recurrent Weights: 1200×150; Bias: 1200×1
3	BiLSTM with 128 hidden units	256	Input weights: 1024×300; Recurrent Weights: 1024×128; Bias: 1024×1
4	Fully connected layer	6	Weights: 6×256; Bias: 6×1
5	Softmax	6	–
6	Classification output (crossentropy)	–	–

Results

Figures 8-11 show confusion matrices which are the classic prediction evaluation tool for classification problems. Figure 8 shows the training set confusion matrix for the case of an LSTM network processing the raw ECG signal. If all the cases were classified correctly, all the fields of the matrix arranged diagonally would contain 1080. Figure 7 corresponds with Figures 4 and 5. Figure 9 shows the confusion matrix of the test set for the case of an LSTM network processing the raw ECG signal. As you can also see in this case, many tested signals were misinterpreted. However, it can be seen that for Brachycardia and Trachycardia, 100% correct classifications were obtained. This is quite surprising because the test set, as one that does not participate in the training process, is usually more difficult to correctly interpret by the neural network. In this case, it was probably different due to the small number of this set (only 60 test signals).

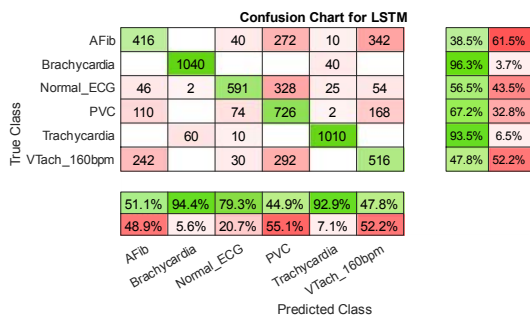


Fig. 8. Confusion matrix for the training set with a raw ECG signal

Figure 10 shows the confusion matrix for the training set after features extraction. Comparing this matrix with the matrix in Figure 8, a fundamental difference can be noticed. It turned out that after extracting the FI and SE features, the prediction accuracy increased significantly. In most of the diseases detected, it is 100%. Only 0.2% of the cases were wrongly assigned by the LSTM network as PVC instead of Normal_ECG. Figure 10 corresponds with Figures 6 and 7.

The curve is hyperbolic. Although there are significant fluctuations initially, the line smoothes over time and eventually reaches an asymptote. Proper data preparation plays an important role. In the discussed case, oversampling was used as part of data preprocessing. The reason was the large variation in the number of ECG signals available to researchers. The entire data pool was 3121. The largest number of reference signals, as many as 1140, related to Normal_ECG. It was the best for Brachycardia - only 60. As the formal requirement for the proper training of the LSTM network was to equalize the number of signals for each of the 6 classes, it was decided that all signals would be duplicated to obtain the number 1140. This was the oversampling used in the research.

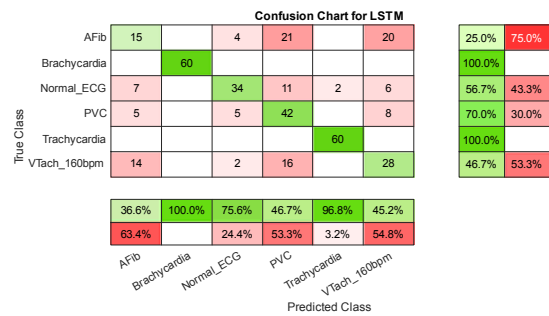


Fig. 9. Confusion matrix for the testing set with a raw ECG signal

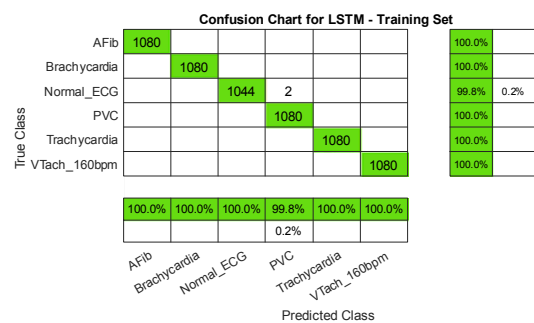


Fig. 10. Confusion matrix for the training set after features extraction

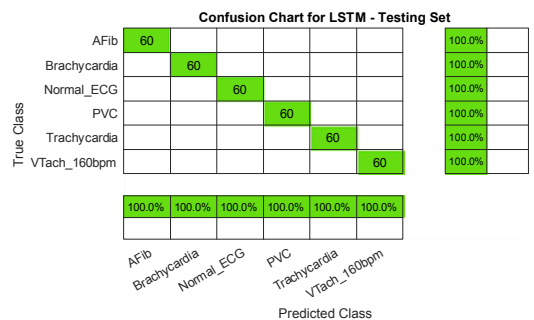


Fig. 11. Confusion matrix for the testing set after features extraction

Finally, Figure 11 shows the confusion matrix for the test set after features extraction. As can be seen, the transformation of a single ECG signal into the two features IF and SE made it possible to achieve the remarkable result of 100% accuracy for all disease categories.

Conclusions and discussion

The results of the conducted research prove that appropriate preprocessing (oversampling) and feature extraction using spectral analysis and Fourier transforms significantly improve the efficiency of LSTM neural network classification in the problem of identifying cardiovascular diseases. Research similar to that described in this publication was conducted by researchers such as Salem, Taheri and Yuan [25] who applied Fourier Transform Spectrograms on the LSTM network achieved 97.2% accuracy. Other interesting examples of the use of the Wavelet Transform in the classification of ECG signals are the studies of W. Zhao et al., 2019 [26], Yildirim Özal, 2018 [27], Isasi et al., 2019 [28]. Accuracy achieved reaches 99.4%.

Authors: Grzegorz Kłosowski, Ph.D. Eng., Lublin University of Technology, Nadbystrzycka 38A, Lublin, Poland, E-mail: g.klosowski@pollub.pl;

Tomasz Rymarczyk, Ph.D. Eng., University of Economics and Innovation, Projektowa 4, Lublin, Poland, E-mail: tomasz.rymarczyk@netrix.com.pl;

Dariusz Wójcik, Research & Development Centre Netrix S.A., Lublin, Poland, E-mail: dariusz.wojcik@netrix.com.pl;

Tomasz Cieplak, Ph.D., Lublin University of Technology, Nadbystrzycka 38A, Lublin, Poland, E-mail: t.cieplak@pollub.pl;

Przemysław Adamkiewicz, Ph.D., University of Economics and Innovation, Projektowa 4, Lublin, Poland,

E-mail: przemyslaw.adamkiewicz@netrix.com.pl.

REFERENCES

- [1] Attia Z. I. et al., An artificial intelligence-enabled ECG algorithm for the identification of patients with atrial fibrillation during sinus rhythm: a retrospective analysis of outcome prediction, *Lancet*, 394 (2019), No. 10201, 861–867
- [2] Chen Y., Ota L., Yu, K., Dong M., Robust activity recognition for aging society, *IEEE J. Biomed. Heal. Informatics*, 22 (2018), No. 6, 1754–1764
- [3] Chen X. et al., IDiSC: A New Approach to IoT-Data-Intensive Service Components Deployment in Edge-Cloud-Hybrid System, *IEEE Access*, 7 (2019), 59172–59184
- [4] Gravina R., Alinia P., Ghasemzadeh H., Fortino G., Multi-sensor fusion in body sensor networks: State-of-the-art and research challenges, *Inf. Fusion*, 35 (2017), 1339–1351
- [5] Qiu H., Qiu M., Lu Z., Selective encryption on ECG data in body sensor network based on supervised machine learning, *Inf. Fusion*, 55 (2020), 59–67
- [6] Arsene C. T. C., Hankins R., Yin H., Deep learning models for denoising ECG signals, in *European Signal Processing Conference*, 2019, vol. 2019-September.
- [7] Mostayed A., Luo J., Shu X., Wee W., Classification of 12-Lead ECG Signals with Bi-directional LSTM Network, 05-Nov-2018. [Online]. Available: <http://arxiv.org/abs/1811.02090>. [Accessed: 02-Feb-2020]
- [8] Saadatnejad S., Oveisi M., Hashemi M., LSTM-Based ECG Classification for Continuous Monitoring on Personal Wearable Devices, *IEEE J. Biomed. Heal. Informatics*, pp. 1–1, May 2019
- [9] Filipowicz S.F., Rymarczyk T., The Shape Reconstruction of Unknown Objects for Inverse Problems, *Przegląd Elektrotechniczny*, 88 (2012), No 3A, 55-57
- [10] Rymarczyk T., Adamkiewicz P., Duda K., Szumowski J., Sikora J., New Electrical Tomographic Method to Determine Dampness in Historical Buildings, *Archives of Electrical Engineering*, 65 (2016), No 2, 273-283
- [11] Rymarczyk T., New Methods to Determine Moisture Areas by Electrical Impedance Tomography, *International Journal of Applied Electromagnetics and Mechanics*, 52 (2016), 79-87
- [12] Rymarczyk T., Using electrical impedance tomography to monitoring flood banks, *International Journal of Applied Electromagnetics and Mechanics*, 45 (2014), 489–494
- [13] Rymarczyk T., Kłosowski G., Innovative methods of neural reconstruction for tomographic images in maintenance of tank industrial reactors. *Eksplotacja i Niezawodność – Maintenance and Reliability*, 21 (2019); No. 2, 261–267
- [14] Rymarczyk T., Sikora J., Waleska B.: Coupled Boundary Element Method and Level Set Function for Solving Inverse Problem in EIT, 7th World Congress on Industrial Process Tomography, WC IPT7, 312-319, 2-5 September 2013, Krakow, Poland
- [15] Kłosowski G., Rymarczyk T., Kania K., Świć A., Cieplak T., Maintenance of industrial reactors based on deep learning driven ultrasound tomography, *Eksplotacja i Niezawodność – Maintenance and Reliability*; 22 (2020), No 1, 138–147
- [16] Grudzien, K.; Chaniecki, Z.; Romanowski, A.; Sankowski, D.; Nowakowski, J.; Niedostatkiewicz, M. Application of twin-plane ECT sensor for identification of the internal imperfections inside concrete beams. In *Proceedings of the 2016 IEEE International Instrumentation and Measurement Technology Conference Proceedings*, Taipei, Taiwan, 23–26 May 2016; 1–6
- [17] Romanowski, A. Big Data-Driven Contextual Processing Methods for Electrical Capacitance Tomography. *IEEE Trans. Ind. Informatics*, 15 (2019), 1609–1618
- [18] Szczesny, A.; Korzeniewska, E. Selection of the method for the earthing resistance measurement. *Przegląd Elektrotechniczny*, 94 (2018), 178–181
- [19] Galazka-Czarnecka, I.; Korzeniewska E., Czarnecki A. et al., Evaluation of Quality of Eggs from Hens Kept in Caged and Free-Range Systems Using Traditional Methods and Ultra-Weak Luminescence, *Applied sciences-basel*, 9 (2019), No. 12, 2430
- [20] Kosinski, T.; Obaid, M.; Wozniak, P.W.; Fjeld, M.; Kucharski, J. A fuzzy data-based model for Human-Robot Proxemics. In *Proceedings of the 2016 25th IEEE International Symposium on Robot and Human Interactive Communication (RO-MAN)*, New York, NY, USA, 26–31 August 2016; 335–340
- [21] Fraczyk, A.; Kucharski, J. Surface temperature control of a rotating cylinder heated by moving inductors. *Appl. Therm. Eng.* 2017, 125, 767–779
- [22] Majchrowicz M., Kapusta P., Jackowska-Strumiłło L., Sankowski D., Acceleration of image reconstruction process in the electrical capacitance tomography 3d in heterogeneous, multi-gpu system, *Informatyka, Automatyka, Pomiary w Gospodarce i Ochronie Środowiska (IAPGOŚ)*, 7 (2017), No. 1, 37-41
- [23] Goetzke-Pala A., Hoła A., Sadowski Ł., A non-destructive method of the evaluation of the moisture in saline brick walls using artificial neural networks. *Archives of Civil and Mechanical Engineering*, 18 (2018), No 4, 1729-1742
- [24] Kozłowski E., Mazurkiewicz D., Żabiński T., Prucnal S., Sęp J., Assessment model of cutting tool condition for real-time supervision system, *Eksplotacja i Niezawodność – Maintenance and Reliability*, 21 (2019); No 4, 679–685
- [25] Salem M., Taheri S., Yuan J. S., ECG Arrhythmia Classification Using Transfer Learning from 2- Dimensional Deep CNN Features, in *2018 IEEE Biomedical Circuits and Systems Conference, BioCAS 2018 - Proceedings*, 2018
- [26] Zhao W. et al., Deep Learning Based Patient-Specific Classification of Arrhythmia on ECG signal, in *Proceedings of the Annual International Conference of the IEEE Engineering in Medicine and Biology Society, EMBS*, 2019, 1500–1503
- [27] Yildirim Ö., A novel wavelet sequences based on deep bidirectional LSTM network model for ECG signal classification, *Comput. Biol. Med.*, 96 (2018), 189–202
- [28] Isasi I. et al., A Robust Machine Learning Architecture for a Reliable ECG Rhythm Analysis during CPR, in *Proceedings of the Annual International Conference of the IEEE Engineering in Medicine and Biology Society, EMBS*, 2019, 1903–1907